Stroke

BASIC AND TRANSLATIONAL SCIENCES

CCR5 Activation Promotes NLRP1-Dependent Neuronal Pyroptosis via CCR5/PKA/CREB Pathway After Intracerebral Hemorrhage

Jun Yan, MD, PhD*; Weilin Xu, MD, PhD*; Cameron Lenahan, BS; Lei Huang, MD; Jing Wen, MD, PhD; Gaigai Li, MD; Xin Hu, MD, PhD; Wen Zheng, MD; John H. Zhang, MD, PhD; Jiping Tang, MD

BACKGROUND AND PURPOSE: Neuronal pyroptosis is a type of regulated cell death triggered by proinflammatory signals. CCR5 (C-C chemokine receptor 5)-mediated inflammation is involved in the pathology of various neurological diseases. This study investigated the impact of CCR5 activation on neuronal pyroptosis and the underlying mechanism involving cAMP-dependent PKA (protein kinase A)/CREB (cAMP response element binding)/NLRP1 (nucleotide-binding domain leucine-rich repeat pyrin domain containing 1) pathway after experimental intracerebral hemorrhage (ICH).

METHODS: A total of 194 adult male CD1 mice were used. ICH was induced by autologous whole blood injection. Maraviroc (MVC)—a selective antagonist of CCR5—was administered intranasally 1 hour after ICH. To elucidate the underlying mechanism, a specific CREB inhibitor, 666-15, was administered intracerebroventricularly before MVC administration in ICH mice. In a set of naive mice, rCCL5 (recombinant chemokine ligand 5) and selective PKA activator, 8-Bromo-cAMP, were administered intracerebroventricularly. Short- and long-term neurobehavioral assessments, Western blot, Fluoro-Jade C, terminal deoxynucleotidyl transferase dUTP nick end labeling (TUNEL), and immunofluorescence staining were performed.

RESULTS: The brain expression of CCL5 (chemokine ligand 5), CCR5, PKA-Cα (protein kinase A-Cα), p-CREB (phospho-cAMP response element binding), and NLRP1 was increased, peaking at 24 hours after ICH. CCR5 was expressed on neurons, microglia, and astrocytes. MVC improved the short- and long-term neurobehavioral deficits and decreased neuronal pyroptosis in ipsilateral brain tissues at 24 hours after ICH, which were accompanied by increased PKA-Cα and p-CREB expression, and decreased expression of NLRP1, ASC (apoptosis-associated speck-like protein containing a CARD), C-caspase-1, GSDMD (gasdermin D), and IL (interleukin)-1β/IL-18. Such effects of MVC were abolished by 666-15. At 24 hours after injection in naive mice, rCCL5 induced neurological deficits, decreased PKA-Cα and p-CREB expression in the brain, and upregulated NLRP1, ASC, C-caspase-1, N-GSDMD, and IL-1β/IL-18 expression. Those effects of rCCL5 were reversed by 8-Bromo-cAMP.

CONCLUSIONS: CCR5 activation promoted neuronal pyroptosis and neurological deficits after ICH in mice, partially through the CCR5/PKA/CREB/NLRP1 signaling pathway. CCR5 inhibition with MVC may provide a promising therapeutic approach in managing patients with ICH.

GRAPHIC ABSTRACT: An online graphic abstract is available for this article.

Key Words: cerebral hemorrhage ■ chemokine receptor ■ inflammasome ■ neuron ■ pyroptosis

Intracerebral hemorrhage (ICH) accounts for 10% to 15% of all strokes worldwide and is a devastating subtype associated with a high mortality and morbidity.[1] Following the initial insult, the secondary brain injury of ICH contributes to the poor outcomes, for which there is no effective therapy.[2] Neuroinflammation plays a critical

Correspondence to: Jun Yan, MD, PhD, Guangxi Medical University Cancer Hospital, Nanning, China. Email yanjun@gxmu.edu.cn
*J. Yan and W. Xu contributed equally.
Supplemental Material is available with this article at https://www.ahajournals.org/doi/suppl/10.1161/STROKEAHA.120.033285.
For Sources of Funding and Disclosures, see page 4031.

Stroke is available at www.ahajournals.org/journal/str

Nonstandard Abbreviations and Acronyms

CCL5	C-C chemokine ligand 5
CCR5	C-C chemokine receptor type 5
CREB	cAMP response element binding protein
GSDMD	gasdermin D
ICH	intracerebral hemorrhage
IL	interleukin
MVC	maraviroc
NLRP1	nucleotide-binding domain leucine-rich repeat pyrin domain containing 1
PKA	protein kinase A
rCCL5	recombinant C-C chemokine ligand 5

role in the pathogenesis of secondary brain injury.[3] However, the molecular mechanisms underlying inflammation-induced neuronal cell death are complex and poorly understood in the setting of ICH.

Inflammasome-mediated regulated cell death, namely pyroptosis, is identified as an important mechanism of inflammation-induced neuronal cell death in a variety of neurological diseases.[4] NLRP1 (nucleotide-binding domain leucine-rich repeat pyrin domain containing 1) is an NLR family member. A wealth of literature suggests that NLRP1 inflammasomes are important drivers of the caspase-1 cleavage. The activated caspase-1 subsequently promotes the maturation and release of proinflammatory IL (interleukin)-1β and IL-18 via formation of plasma membrane pores, namely, cell pyroptosis.[5] In the brain, NLRP1 inflammasomes are primarily expressed by neurons.[5] Thus, targeting NLRP-1 inflammasome-mediated neuronal pyroptosis may provide new insight and a theoretical basis for developing an effective treatment for ICH.

CCR5 (C-C chemokine receptor 5) is a 7-transmembrane G-protein–coupled receptor that participates in leukocyte recruitment to areas of tissue damage during inflammatory responses and has been shown to be a viable target of anti-inflammatory therapy. Maraviroc (MVC)—an Food and Drug Administration–approved selective CCR5 antagonist for patients with HIV—improved outcomes in animal models of immune-mediated acute and chronic tissue inflammation.[6] Recent studies have also demonstrated that CCR5 inhibition promoted early recovery of motor function after traumatic brain injury and cerebral ischemia in rodents.[7] Interestingly, the CREB (cAMP response element binding) protein is reportedly one of the downstream pathway proteins involved in CCR5 signaling.[8] The downregulation of neuronal CCR5 in mice with HIV enhanced the plasticity of cortical neurons and the recovery of learning and memory function by increasing CREB protein level.[8] The cAMP-dependent PKA (protein kinase A) is a vital kinase in CREB activation[9] that phosphorylates CREB at the serine 133 site. The active CREB further activated the gene-related synaptic plasticity responsible for participating in long-term memory formation.[9] Although CREB often promotes anti-inflammatory immune responses,[10] its effects on NLRP1 inflammasome have not been explored.

In the current study, we hypothesized that the activation of CCR5 promoted NLRP1-mediated pyroptosis after ICH. MVC-mediated CCR5 inhibition would attenuate neurological deficits and decrease NLRP1-dependent neuronal pyroptosis through activation of the PKA/CREB signaling pathway after ICH in mice.

METHODS

The data that support the findings of this study are available from the corresponding author upon reasonable request. Detailed description of the Materials and Methods is provided in Methods in the Supplemental Material. The authors declare that all supporting data are available within the article and the Supplemental Material. We provide the detailed statistics in the Data Set in the Supplemental Material. All experimental protocols and procedures were approved by the Ethics Committee of the Guangxi Medical University, and in accordance with the National Institutes of Health guidelines.

RESULTS

Animal Mortality and Exclusion

The overall mortality was 5.15% (10/194). None of the sham-operated mice died in this study. The mortality did not significantly differ among the experimental ICH groups. None of the ICH mice were excluded (Table I in the Supplemental Material). No significant adverse effects were observed in treatment groups.

Time Course and Spatial Expression of CCR5 in Brain After ICH

ELISA and Western blot were performed to assess the expression of CCL5 (chemokine ligand 5), CCR5, PKA-Cα (protein kinase A-Cα), p-CREB (phospho-cAMP response element binding), and NLRP1 at 0, 3, 6, 12, 24, and 72 hours in the ipsilateral (right) cerebral hemispheres after ICH. Compared with the sham group, there was a notable elevation of CCL5 levels detected at 3 hours (16.78±3.02 versus 8.61±2.97; $P<0.001$), which was determined by ELISA to be at a relatively high level at 24 hours (20.69±2.99 versus 8.61±2.97; $P<0.001$). CCR5 levels were significantly increased at 3 hours (1.04±0.16 versus 0.59±0.04; $P<0.001$), which peaked at 24 hours (1.29±0.19 versus 0.59±0.04; $P<0.001$), and started to decrease at 72 h (0.68±0.11 versus 0.59±0.04; $P=0.64$) after ICH (Figure 1A).

PKA-Cα and p-CREB—the potential downstream proteins of CCR5—were also elevated temporarily after ICH in a similar pattern to CCR5. NLRP1 inflammasome expression was significantly upregulated at 6 hours

 Stroke. 2021;52:4021–4032. DOI: 10.1161/STROKEAHA.120.033285

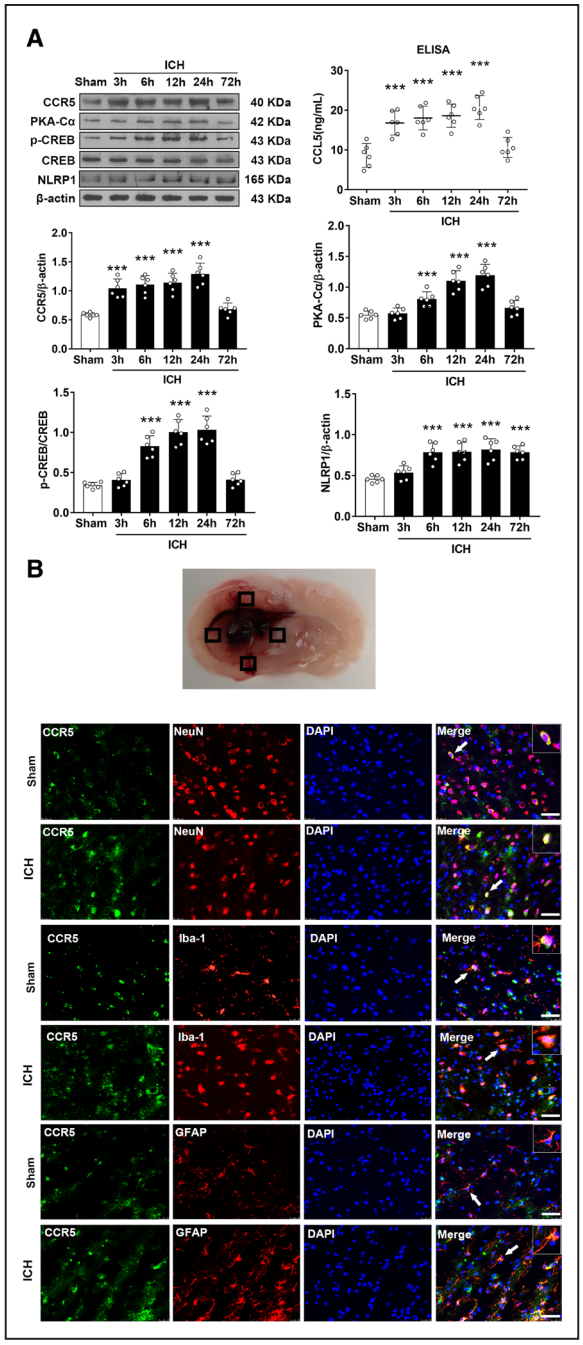

Figure 1. Time course of CCL5 (chemokine ligand 5), CCR5 (C-C chemokine receptor 5), PKA-Cα (protein kinase A-Cα), p-CREB (phospho-cAMP response element binding), CREB (cAMP response element binding), and NLRP1 (nucleotide-binding domain leucine-rich repeat pyrin domain containing 1) protein levels after intracerebral hemorrhage (ICH).

A, Representative Western blot images, ELISA, and quantitative analyses of CCL5, CCR5, PKA-Cα, p-CREB, CREB, and NLRP1 at 3, 6, 12, 24, and 72 h after ICH. n=6 per group. Data are represented as mean±SD. **P*<0.05, ***P*<0.01, ****P*<0.001 vs sham. For proteins with similar molecular weights, namely, PKA-Cα (42 KDa) vs β-actin (43 KDa), we used the same blots following Western blot membrane stripping for restaining protocol. **B**, Double immunofluorescence staining showed CCR5 (green) colocalized with neuron (neuronal nuclear [NeuN], red), microglia (IBA-1 [ionized calcium-binding adaptor molecule 1], red) and astrocytes (GFAP [glial fibrillary acidic protein], red) in the perihematomal area in sham group and ICH (24 h) group. The small black squares in the coronal section of brain indicated the area where microphotograph was taken. Scale bar, 50 μm. n=2/group. DAPI indicates 4′,6-diamidino 2-phenylindole.

(0.78±0.11 versus 0.46±0.04; *P*<0.001) and peaked at 72 hours (0.78±0.08 versus 0.46±0.04; *P*<0.001) after ICH when compared with the sham group (Figure 1A).

Double immunofluorescence staining revealed that CCR5 was mainly expressed on the neurons, microglia, and astrocytes of the ipsilateral basal cortex at 24 hours after ICH (Figure 1B).

Inhibition of CCR5 With MVC Attenuated Neurobehavioral Deficits at 24 and 72 Hours After ICH

There was no significant difference of baseline performances among the modified Garcia, forelimb placement, and corner turn tests. At 24 hours after ICH, there were significant neurological impairments in the ICH+vehicle group when compared with the Sham group (10.33±2.07 versus 20±0.89, *P*<0.001; 6.67±8.17 versus 75±10.49, *P*<0.001; 51.67±7.53 versus 5.00 [0–10], *P*=0.002; Figure 2A). MVC treatment at doses of 150 and 450 μg/kg per day significantly improved the neurological performance in the modified Garcia test (16.5±1.05 and 16.17±1.47 versus 20±0.89; *P*<0.001), forelimb placement test (35±10.49 and 38.33±9.83 versus 75±10.49; *P*<0.001), and corner turn test (20±8.94 and 18.33±7.53 versus 5.00 [0–10]; *P*=0.017 and *P*=0.019) at 24 hours after ICH compared with the vehicle-treated ICH group (Figure 2A).

Based on this result, the dosage of 150 μg/kg/day was determined to be the best dose of MVC and was used in subsequent experiments. Consistently, MVC (150 μg/kg per day) treatment significantly decreased neurobehavioral deficits in ICH mice when compared with the ICH+vehicle group (14.0±1.27 versus 10.67±1.21, *P*<0.001; 36.67±10.33 versus 6.67±8.17, *P*<0.001; 26.67±10.33 versus 0 [0–10], *P*=0.008; Figure 2B) at 72 hours after ICH. Conversely, the first administration of MVC (150 μg/kg per day) at 24 hours after ICH did not significantly decrease neurobehavioral deficits in ICH mice compared with the ICH+vehicle group (10.50±1.05 versus 10.33±1.03, *P*=0.95; 11.67±7.53 versus 8.33±7.53, *P*=0.73; 8.33±7.53 versus 5 [0–10], *P*=0.99; Figure 2C) at 72 hours after ICH.

MVC-Mediated Inhibition of CCR5 Reduced Neuronal Pyroptotic Cell Death at 24 Hours After ICH

Terminal deoxynucleotidyl transferase dUTP nick end labeling (TUNEL) staining and Fluoro-Jade C staining were each used to assess whether MVC treatment reduced neuronal cell death. Specifically, costaining of neuronal marker, neuronal nuclear (NeuN), with the cleaved caspase-1 was used to assess neuronal pyroptosis 24 hours after ICH. TUNEL-positive neurons (34.83±4.31 versus 3.5±2.17; *P*<0.001) and

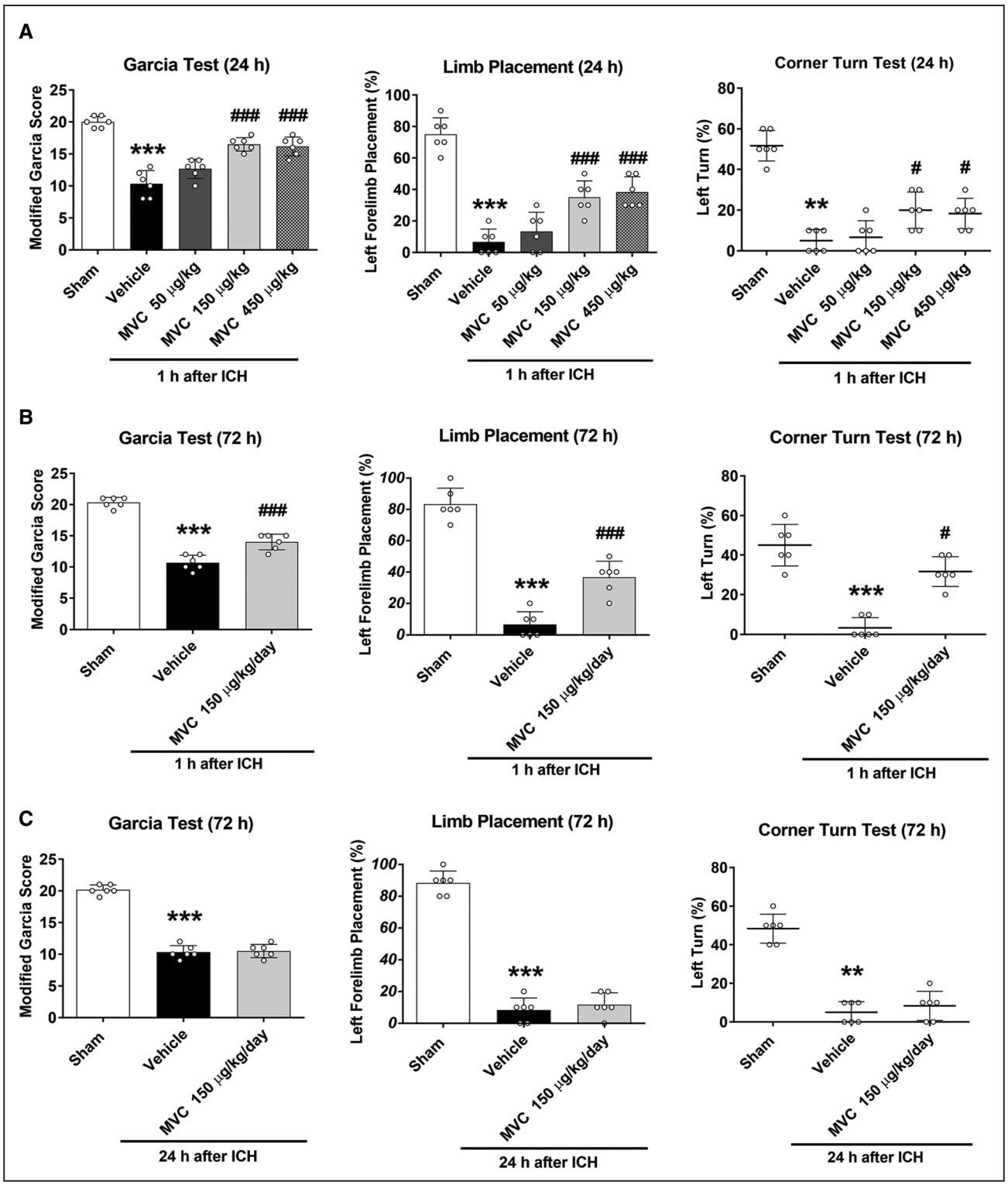

Figure 2. The effects of maraviroc (MVC) on neurobehavior outcomes at 24 and 72 h after intracerebral hemorrhage (ICH). **A**, Modified Garcia, forelimb placement, and corner turn tests at 24 h after ICH for administration of Maraviroc at 1 h after ICH. **B**, Modified Garcia, forelimb placement, and corner turn test at 72 h after ICH for administration of Maraviroc at 1 h after ICH. **C**, Modified Garcia, forelimb placement, and corner turn test at 72 h after ICH for the first treatment with administration of Maraviroc at 24 h after ICH. n=6 per group. Data are represented as mean±SD or median (interquartile range). **P*<0.05, ***P*<0.01, ****P*<0.001 vs sham, #*P*<0.05 ##*P*<0.01, ###*P*<0.001 vs ICH+vehicle.

the Fluoro-Jade C-positive degenerating neurons (278.30±37.64 versus 37.83±24.13; *P*<0.001) in ICH rats were significantly increased compared with the Sham group at 24 hours after ICH (Figure 3A and 3B). MVC-mediated inhibition of CCR5 significantly reduced the number of TUNEL-positive neurons (25.83±4.26

 Stroke. 2021;52:4021–4032. DOI: 10.1161/STROKEAHA.120.033285

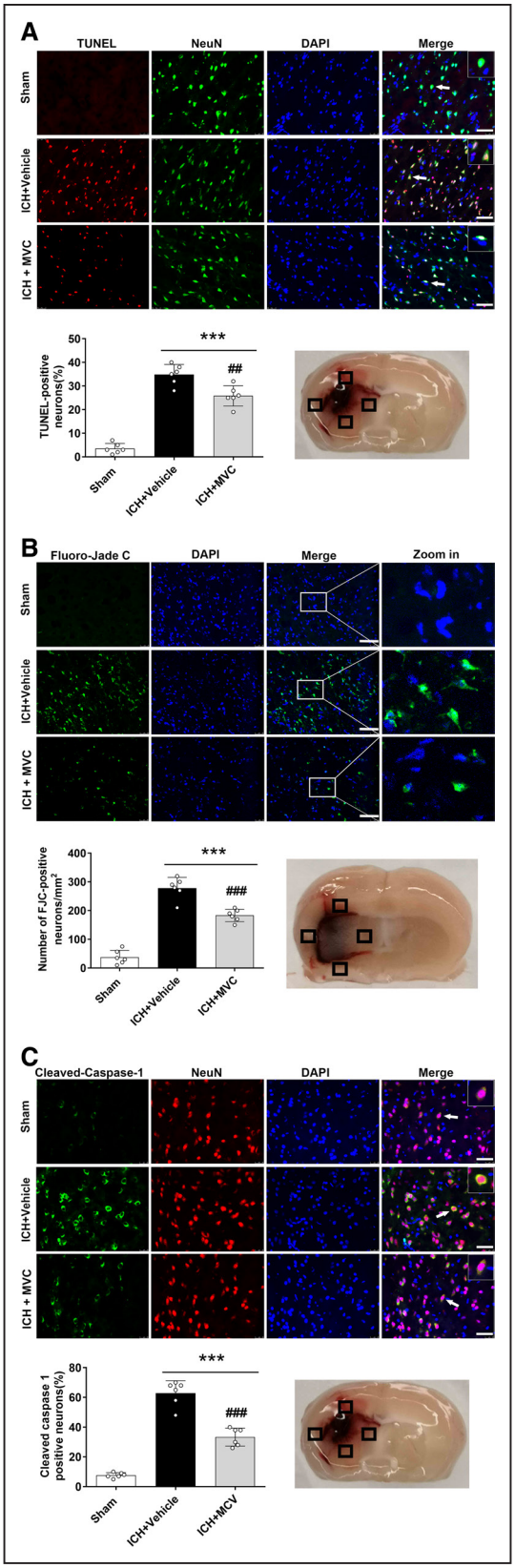

Figure 3. The effects of CCR5 (C-C chemokine receptor 5) inhibition with maraviroc (MVC) on neuronal damage including pyroptosis at 24 h after intracerebral hemorrhage (ICH). **A**, Representative microphotographs and quantitative analysis of terminal deoxynucleotidyl transferase dUTP nick end labeling (TUNEL)-positive neurons in the perihematomal area (*Continued*)

versus 34.83±4.31; *P*=0.002) and Fluoro-Jade C-positive degenerating neurons (183.30±21.60 versus 278.30±37.64; *P*=0.001; Figure 3A and 3B).

Additionally, there were significantly more cleaved caspase-1–positive neurons in the perihematomal region at 24 hours after ICH in the ICH+vehicle group when compared with the sham group (62.83±8.40 versus 7.67±1.75; *P*<0.001), suggesting increased neuronal pyroptosis. MVC treatment significantly reduced the number of cleaved caspase-1–positive neurons in the perihematomal region at 24 hours after ICH when compared with the ICH+vehicle group (33.33±6.02 versus 62.83±8.40; *P*<0.001; Figure 3C). In the experiments with the injection of recombinant CCL5, the rCCL5 induced neuronal death and neuronal pyroptosis (Figure VII in the Supplemental Material).

MVC Improved Long-Term Sensorimotor Coordination, Spatial Learning, and Reference Memory Functions, as Well as Reduced Hippocampal Cornu Ammonis 1 (CA1) Neuronal Loss After ICH

Baseline performance was not significantly different regarding foot fault and rotarod tests among the mice. Compared with the sham group, the ICH+vehicle group had more foot faults of the left forelimb in the foot fault test (37.75±2.77 versus 3.5±1.19, *P*<0.001; 23.25±3.73 versus 3.63±1.60, *P*<0.001; 11.88±2.90 versus 3.75±1.49, *P*<0.001) and shorter latency to fall in the rotarod test (16.63±3.89 versus 42.38±4.93, *P*<0.001; 20.88±4.09 versus 43.88±7.02, *P*<0.001; 20.13±4.29 versus 46.88±6.66, *P*<0.001) at the first, second, and third weeks after ICH (Figure 4A). MVC treatment significantly decreased foot faults of the left forelimb (12±3.62 versus 37.75±2.77, *P*<0.001; 11.5±2.45 versus 23.25±3.73, *P*<0.001; 5.62±1.92 versus 11.88±2.90, *P*<0.001; Figure 4A), but increased falling latency in ICH mice (28.13±7.59 versus 16.63±3.89, *P*=0.001; 31.13±8.34 versus 20.88±4.09, *P*=0.005; 33.25±7.56 versus 20.13±4.29, *P*<0.001; Figure 4A).

In the Morris water maze test, the ICH+vehicle group showed significantly longer swim distance and escape latency compared with the sham group. However, the MVC treatment significantly decreased the escape latency and swim distance on blocks 3 to 5 compared with the ICH+vehicle group (*P*<0.001; Figure 4A). In the probe

Figure 3 Continued. 24 h after ICH. **B**, Representative microphotographs and quantitative analysis of Fluoro-Jade C-positive degenerating neurons in the perihematomal area at 24 h after ICH. **C**, Representative microphotographs and quantitative analysis of cleaved caspase-1 (C-caspase-1)–positive neurons in the perihematomal area. The small black square in the coronal section of the brain indicated the area where the microphotograph was taken. Scale bar, 50 μm. n=6 per group. Data are represented as mean±SD. DAPI indicates 4′,6-diamidino 2-phenylindole; and NeuN, neuronal nuclear. **P*<0.05, ***P*<0.01, ****P*<0.001 vs sham, #*P*<0.05, ##*P*<0.01, ###*P*<0.001 vs ICH+vehicle.

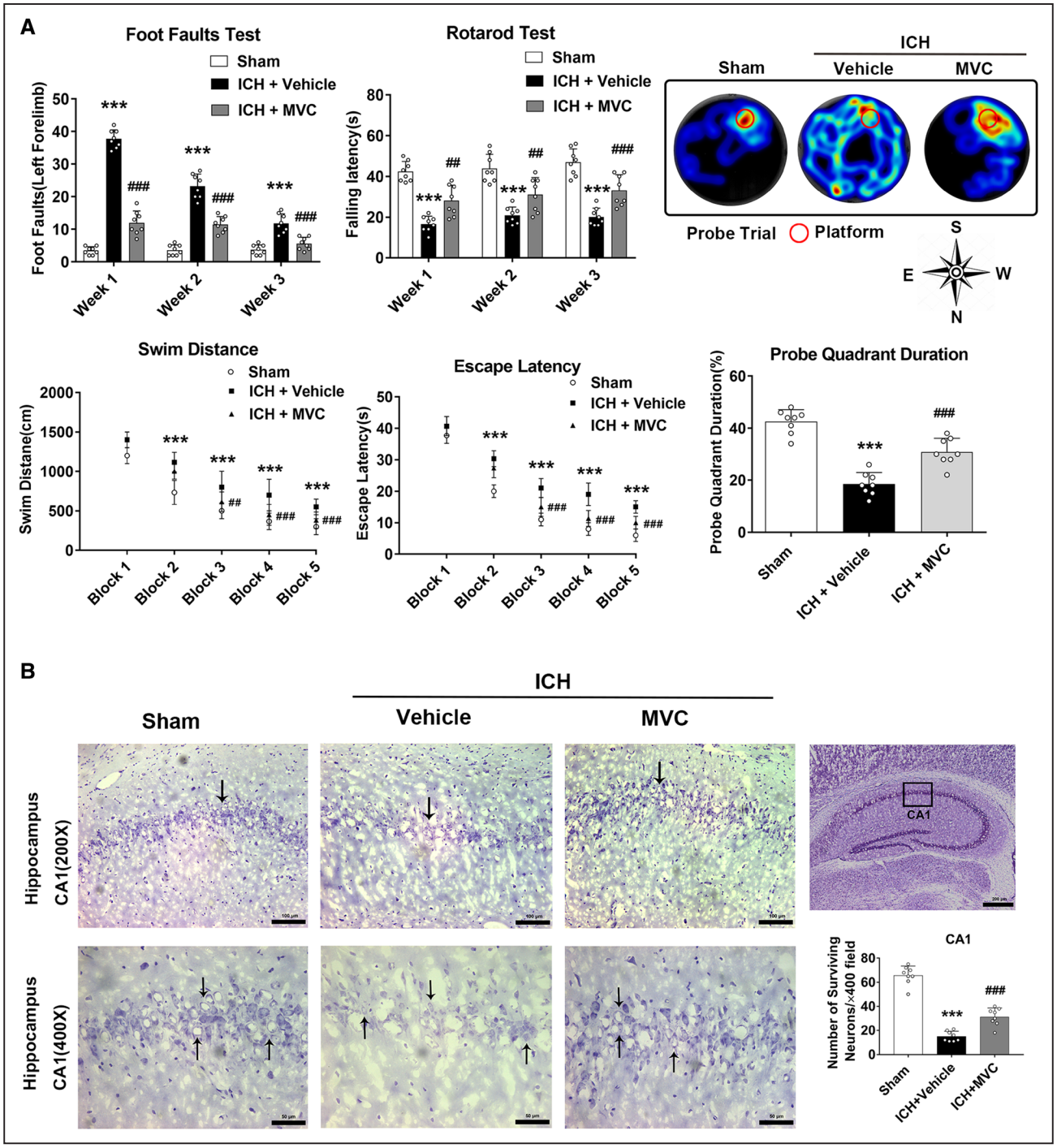

Figure 4. Maraviroc (MVC) improved long-term neurobehavioral function after intracerebral hemorrhage (ICH).
A, Foot fault test and Rotarod test on 1, 2, and 3 wk after ICH. Escape latency and swim distance of Morris water maze on 21 to 25 d after ICH. Representative heat map in probe test and probe quadrant duration on day 25 post-ICH. **B**,The MVC post-treatment attenuated the neuronal loss of hippocampus cornu ammonis 1 (CA1) at day 25 after ICH in mice. Nissl staining showed that ICH increased the neuronal loss in the hippocampus CA1 region, but MVC treatment attenuated the neuronal loss. Arrows indicated the normal neurons. n=8 per group. **P*<0.05, ***P*<0.01, ****P*<0.001 vs sham group; #*P*<0.05, ##*P*<0.01, ###*P*<0.001 vs ICH+vehicle group. Scale bar, 200 μm (general), 100 μm (regions) and 50 μm (regions). Data are represented as mean±SD.

quadrant trial, the ICH+vehicle group spent less time in the target quadrant compared with the sham group (18.50±4.41 versus 42.5±4.60; *P*<0.001). However, MVC treatment markedly increased the time spent in the probe quadrant compared with the ICH+vehicle group (30.88±5.22 versus 18.50±4.41; *P*<0.001; Figure 4A).

Nissl staining was conducted to evaluate the neuronal loss in the hippocampal CA1 region on day 25 after ICH. The results revealed that fewer neurons survived in the hippocampal CA1 region in the ICH+vehicle group than the sham group (15.13±4.15 versus 65.75±7.74; *P*<0.001), but MVC treatment significantly increased the

Stroke. 2021;52:4021–4032. DOI: 10.1161/STROKEAHA.120.033285

number of surviving CA1 neurons compared with the ICH+vehicle group (31.38±7.31 versus 15.13±4.15; $P<0.001$; Figure 4B).

CREB Inhibitor Reversed the Neuroprotective Effects of MVC Against Neurobehavioral Deficits and CCR5/PKA Cα/CREB/NLRP1-Mediated Pyroptosis at 24 Hours After ICH

Pretreatment with CREB inhibitor, 666-15, significantly reversed the neurobehavioral benefits of MVC on the modified Garcia (11.0±1.67 versus 16.33±1.86; $P<0.001$), forelimb placement (6.67±8.17 versus 36.67±10.33; $P<0.001$), and corner turn tests (0 [0–10] versus 15.00±10.49; $P=0.03$) at 24 hours after ICH (Figure 5A).

In addition, MVC significantly increased protein levels of PKA-Cα (1.11±0.21 versus 0.65±0.09; $P<0.001$) and p-CREB (1.22±0.24 versus 0.97±0.09; $P=0.02$) but reduced the expression of NLRP1 (0.70±0.11 versus 1.17±0.22; $P<0.001$), ASC (apoptosis-associated speck-like protein containing a CARD; 0.64±0.09 versus 0.91±0.15; $P=0.006$), C-caspase-1 (0.68±0.06 versus 1.07±0.14; $P<0.001$), N-GSDMD (N-gasdermin D; 0.50±0.05 versus 1.06±0.16; $P<0.001$), IL-1β (0.44±0.06 versus 1.06±0.12; $P<0.001$), and IL-18 (0.28±0.02 versus 1.03±0.15; $P<0.001$) within the post-ICH brain tissue of the ipsilateral hemisphere (Figure 5B). Consistently, 666-15 reversed the effect of MVC on cell death and the CCR5/PKA-Cα/CREB/NLRP1 signaling pathway, which were associated with increased protein levels of NLRP1 (1.11±0.18 versus 0.62±0.10), ASC (1.08±0.18 versus 0.65±0.09), C-caspase-1 (1.02±0.13 versus 0.46±0.09), N-GSDMD (0.97±0.09 versus 0.53±0.07), IL-1β (0.87±0.12 versus 0.35±0.04), and IL-18 (1.04±0.16 versus 0.45±0.06) compared with MVC-treated ICH mice ($P<0.001$; Figure 5B).

CCR5 Activation via rCCL5 Resulted in Neurological Deficits and Pyroptosis in Naive Mice Through the CCR5/PKA Cα/CREB/NLRP1 Signaling Pathway at 24 Hours After rCCL5 Injection

The intracerebroventricular injection of rCCL5 significantly reduced neurological scores of the modified Garcia (9.33±1.37 versus 19.17±1.60; $P<0.001$), limb placement (23.33±10.33 versus 90.00±8.94; $P<0.001$), and corner turn tests (18.33±7.52 versus 55.00±10.49; $P<0.001$) in naive mice (Figure 6A) and led to significantly higher protein levels of NLRP1 (0.99±0.18 versus 0.45±0.11), ASC (0.84±0.08 versus 0.21±0.02), C-caspase-1 (1.04±0.15 versus 0.28±0.02), N-GSDMD (1.23±0.19 versus 0.17±0.02), IL-1β (1.01±0.17 versus 0.57±0.03), and IL-18 (1.11±0.13 versus 0.31±0.02) in the ipsilateral brain tissue ($P<0.001$; Figure 6B). Conversely, PKA activator, 8-Bromo-cAMP, reversed the effects of rCCL5 by significantly increasing PKA-Cα expression in the naive+rCCL5+8-Bromo-cAMP group when compared with the naive+rCCL5+vehicle group (1.02±0.19 versus 0.58±0.08; $P<0.001$; Figure 6B).

DISCUSSION

In the present study, we explored the effects of CCR5 antagonist, MVC, on inhibiting NLRP1-mediated pyroptosis through activation of the PKA/CREB signaling pathway in a mouse model of ICH. The novel findings are as follows: (1) the expression of CCR5 and CCL5 and the downstream effectors of PKA Cα, CREB, and NLRP1 were upregulated and peaked at 24 hours after ICH. CCR5 was expressed in neurons, astrocytes, and microglia; (2) intranasal administration of MVC at a dose of 150 μg/kg per day significantly improved short- and long-term neurobehavioral outcomes, reduced neuronal pyroptosis, increased brain expression of PKA-Cα and p-CREB, but decreased expression of NLRP1, ASC, C-caspase-1, N-GSDMD, IL-1β, and IL-18 at 24 hours after ICH. Conversely, the CREB inhibitor reversed these effects of MVC; (3) the activation of brain CCR5 using rCCL5 via intracerebroventricular injection administration resulted in neurological deficits and pyroptosis in naive mice. These detrimental effects in naive mice were abolished significantly by activating brain PKA-Cα using 8-Bromo-cAMP. Collectively, CCR5 activation promotes NLRP1-mediated pyroptosis after ICH, at least partly through the CCR5/PKA/CREB signaling pathways.

Regulated cell death is characterized as any form of cell death caused by an intracellular or extracellular death program, including apoptosis, necroptosis, and pyroptosis. Unlike apoptosis and necroptosis, pyroptosis is a highly inflammatory form of regulated cell death exclusively mediated by cleaved caspase-1.[11] NLRP1 activation promotes inflammasome formation, resulting in the recruitment and activation of caspase-1 via conversion of precursor caspase-1 into cleaved caspase-1. The cleaved caspase-1 further cleaves precursor IL-1β and IL-18 into mature proinflammatory IL-1β and IL-18.[5] Additionally, cleaved caspase-1 is an enzyme specific for cell pyroptosis, which leads to cell membrane pore formation, rapid loss of membrane integrity, and release of proinflammatory intracellular contents.[12] In an animal model of spinal cord injury, the mRNA and protein expression of NLRP1 was significantly elevated from 18 to 24 hours after spinal cord injury.[13] In a cerebral ischemic stroke model, NLRP1 inflammasome expression in the ipsilateral brain tissue increased as early as 1 hour and was maintained at the increased level when measured at 12, 24, and 72 hours after stroke.[14] Consistently, we observed a time-dependent upregulation of endogenous expression of NLRP1 inflammasome in

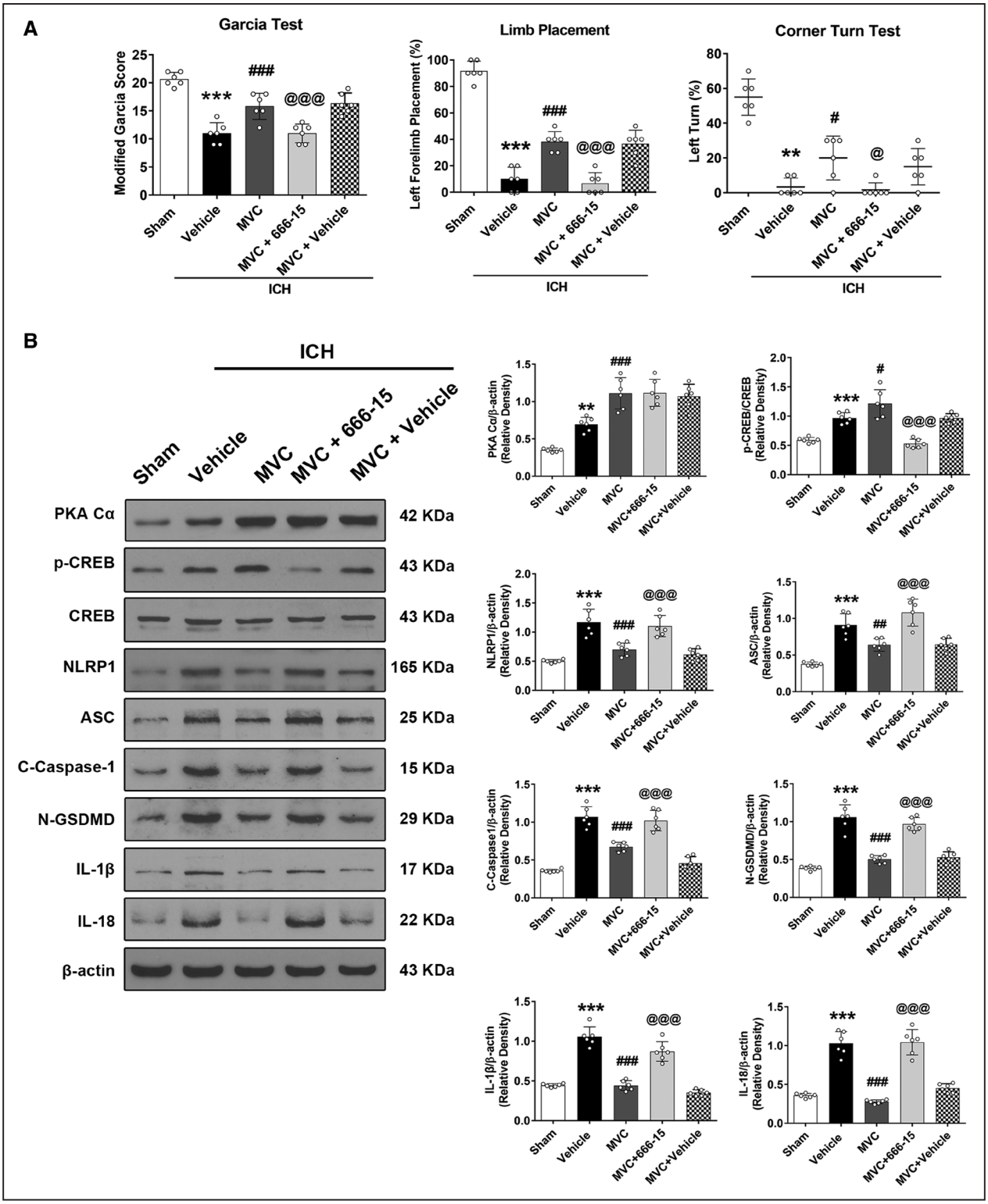

Figure 5. Inhibition of CREB (cAMP response element binding) with 666-15 abolished the neurological function benefit and antineuronal pyroptotic effect of maraviroc (MVC) in intracerebral hemorrhage (ICH) mice.

A, Modified Garcia test. Forelimb placement test. Corner turn test. **B**, Representative Western blot bands. Quantitative analyses of PKA-Cα (protein kinase A-Cα), p-CREB (phospho-cAMP response element binding), NLRP1 (nucleotide-binding domain leucine-rich repeat pyrin domain containing 1), ASC (apoptosis-associated speck-like protein containing a CARD), C-caspase-1, N-GSDMD (N-gasdermin D), IL (interleukin)-1β, and IL-18 in the ipsilateral hemisphere at 24 h after ICH. n=6 per group. Data are represented as mean±SD or median (interquartile range). **P*<0.05, ***P*<0.01, ****P*<0.001 vs sham, #*P*<0.05, ##*P*<0.01, ###*P*<0.001 vs ICH+vehicle, and @*P*<0.05, @@*P*<0.01, @@@*P*<0.001 vs ICH+MVC+vehicle. For proteins with similar molecular weights, namely, PKA-Cα (42 KDa) vs β-actin (43 KDa), we used the same blots following Western blot membrane stripping for restaining protocol.

 Stroke. 2021;52:4021–4032. DOI: 10.1161/STROKEAHA.120.033285

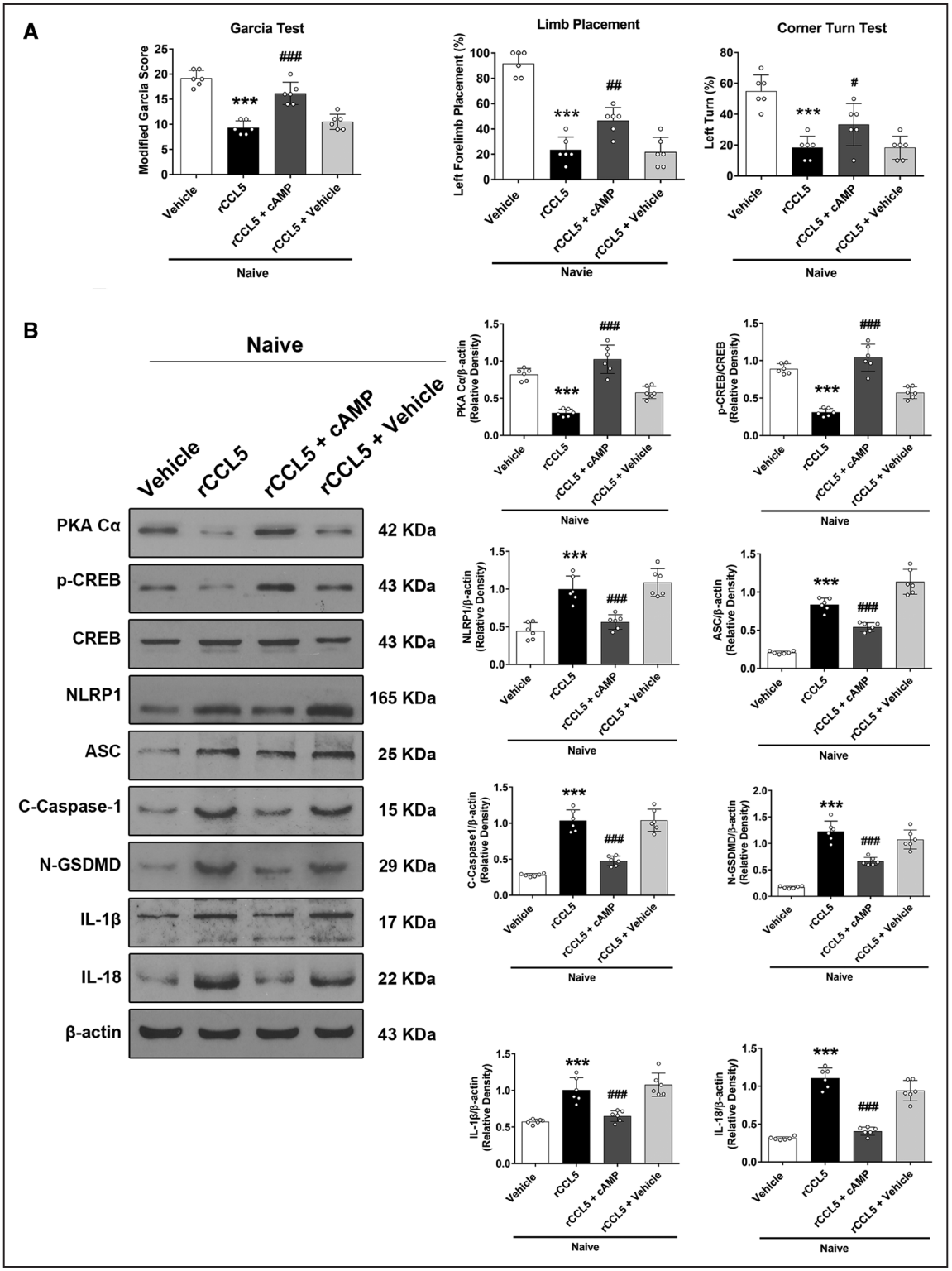

Figure 6. The detrimental effects of rCCL5 (recombinant chemokine ligand 5) in naive mice via activating CCR5 (C-C chemokine receptor 5)/PKA-Cα (protein kinase A-Cα)/CREB (cAMP response element binding)/NLRP1 (nucleotide-binding domain leucine-rich repeat pyrin domain containing 1) signaling pathway.

A, Modified Garcia test, forelimb placement test, and corner turn test. **B**, Representative Western blot bands. Quantitative analyses of PKA-Cα, p-CREB (phospho-cAMP response element binding), NLRP1, ASC (apoptosis-associated speck-like protein containing a CARD), C-Caspase-1, N-GSDMD (N-gasdermin D), IL (interleukin)-1β, and IL-18 in the ipsilateral hemisphere at 24 h after rCCL5 administration in naive mice. n=6 per group. Data are represented as mean±SD. **P*<0.05, ***P*<0.01, ****P*<0.001 vs naive+vehicle, #*P*<0.05, ##*P*<0.01, ###*P*<0.001 vs naive+rCCL5+vehicle. For proteins with similar molecular weights, namely, PKA-Cα (42 KDa) vs β-actin (43 KDa), we used the same blots following Western blot membrane stripping for restaining protocol.

the ipsilateral hemisphere after ICH, which started at 12 hours and peaked at 24 hours after ICH.

CCR5—a chemokine receptor—plays an essential role in mediating leukocyte transport during inflammation. CCR5 was widely expressed in cortex, thalamus, striatum, hippocampus, endothelium, and ependyma.[15] Our present data showed that CCR5 was primarily colocalized with neurons, microglia, and astrocytes within the brain, which coincided with previous studies.[15,16] The CCR5 mRNA and protein levels were increased in brain, spinal cord, and blood plasma at 22 hours after middle cerebral artery occlusion in mice.[17] Consistently, we also observed upregulated protein expression of CCR5 was upregulated at an early stage and peaked at 24 hours after ICH, which accompanied a similar pattern of increased CCL5 ligands, as well as increased protein levels of PKA-Cα, p-CREB, and NLRP1. These results suggested that CCR5 was increased as a response to ICH-induced CCL5 elevation in the acute phase. The upregulation of PKA-Cα and p-CREB may serve as an endogenous neuroprotective mechanism to counteract the deleterious signaling of CCR5 activation and may facilitate homeostatic maintenance in the injured brain. However, such endogenous increases are not sufficient to overcome the effects of CCL5/CCR5 on NLRP1 activation after ICH.

MVC—a novel selective antagonist of CCR5—has been shown to be anti-inflammatory and antiapoptotic in animal models of autoimmune encephalomyelitis and pancreatic cancer.[18,19] However, the effect of MVC-mediated CCR5 inhibition on neuronal pyroptosis has not been elucidated. In this study, we observed that intranasal administration of MVC 1 hour after ICH significantly improved neurological deficits. Based on our results, the treatment of MVC 1 hour after ICH is effective but not at 24 hours. Further studies are needed to further explore the maximum therapeutic window within 24 hours. In addition, MVC inhibited the expression of brain NLRP1 inflammasome, cleaved caspase-1, IL-1β/IL-18β, and pyroptosis marker, N-GSDMD, after ICH. Importantly, immunohistochemical assays showed that MVC reduced the numbers of degenerating neurons, especially cleaved caspase-1–positive neurons after ICH. The antipyroptotic feature of MVC was additional to its antiapoptotic effect. ICH directly damaged the striatal region, resulting in impaired sensorimotor function.[20] In the present study, a battery of neurobehavioral tests, including modified Garcia, limb placement, and corner turn tests, consistently revealed the sensorimotor deficits in mice at 24 and 72 hours post-ICH, which correlated with the neuronal death and loss of neurons in the perihematomal brain tissues. The striatal-associated motor dysfunction remains as shown in the foot fault test and rotarod test at 1, 2, and 3 weeks after ICH in mice. Furthermore, secondary cerebral ischemia may occur in the hippocampal CA1 region post-ICH.[21] Neurons in the hippocampal CA1 region were sensitive to ischemia and were closely related to learning and memory functions of humans and mammals. Nissl staining showed that MVC treatment delayed neuronal death in the hippocampal CA1 region at day 25 after ICH, which is associated with spatial learning deficits identified by the Morris water maze test. Early inhibition of CCL5/CCR5 signaling provided long-term neuronal protection, leading to improved sensorimotor and cognitive dysfunction in ICH mice.

Furthermore, we explored the possible mechanism underlying brain CCR5 activation in NLRP1-mediated pyroptosis after ICH. Previous studies have demonstrated that CCR5 inhibition promoted early recovery of motor function, neuroplasticity, learning, and memory through the CREB signaling pathway in disease models of traumatic brain injury and cerebral ischemia.[7,8] High expression of local CREB significantly improved motor nerve function after cerebral infarction.[22] Our results demonstrated that CCR5 inhibition using MVC significantly increased expression of phosphorylated PKA-Cα and CREB but downregulated NLRP1, ASC, C-caspase-1, N-GSDMD, IL-1β, and IL-18 at 24 hours after ICH. A potent and selective CREB inhibitor 666-15 could decrease CREB activation.[23] In the present study, the application of 666-15 before ICH induction significantly decreased protein levels of p-CREB within ipsilateral brain tissue and reversed the beneficial effects of MVC on neurobehavioral deficits and pyroptosis after ICH. These findings implicated that CREB phosphorylation may be the downstream signal of MVC-mediated CCR5 inhibition responsible for downregulating the NLRP1-dependent neuronal pyroptosis after ICH.

Interestingly, the administration of 666-15 did not alter the MVC-induced brain PKA-Cα upregulation. Although the biological role of PKA-Cα has not been well-defined, it appears to function as a key kinase in activating CREB.[24] We further investigated the role of PKA-Cα in CCR5-mediated pyroptosis and its relationship to CREB activation. Brain CCR5 activation via intracerebroventricular administration of rCCL5 in naive mice decreased the brain expression of PKA-Cα and phosphorylated CREB but upregulated NLRP1, ASC, C-caspase-1, N-GSDMD, as well as IL-1β and IL-18 at 24 hours after rCCL5 injection, leading to significant neurological deficits. The administration of 8-Bromo-cAMP reversed the detrimental effects of rCCL5-mediated CCR5 activation on neurobehavioral function and brain pyroptosis by upregulating the expression of PKA-Cα and p-CREB, suggesting PKA as an upstream signal of CREB activation after ICH. Collectively, our findings reveal that CCR5 activation using rCCL5 promoted pyroptosis, partially through the CCR5/PKA/CREB/NLRP1 signaling pathway.

There are some limitations in this study. First, the present study only focused on pyroptosis after ICH. However, we cannot exclude the contribution of CCR5

 Stroke. 2021;52:4021–4032. DOI: 10.1161/STROKEAHA.120.033285

to apoptosis and the mechanism involving the MAPK (mitogen-activated protein kinase) signaling pathway.[8] Second, we cannot rule out the possibility of NLRP3 signaling in CCR5-mediated pyroptosis after ICH. Microglial NLRP3 inflammasome was significantly upregulated in the mouse model of ICH.[25] CREB phosphorylation negatively regulated the expression of NLRP3-ASC-caspase 1 inflammasome.[26] Nevertheless, the NLRP1 inflammasome is mainly expressed in neurons and is essential for pyroptotic neuronal death,[5] whereas the NLRP3 inflammasome appears to be primarily expressed in microglia and is likely responsible for microglial activation.[27] Third, we used only male mice in this study. Sexual dimorphism exists in neuroinflammation and its mechanisms. Previous studies have shown that female mice are less susceptible to mortality and have improved neurobehavioral outcomes compared with male mice in the setting of ICH.[28] At last, the primary antibody omission control is not the true negative control for validating the antibody specificity, which only controls the nonspecific staining of secondary antibody. The 5 key conceptual pillars were proposed by the International Working Group on Antibody Validation in 2016. The knockout validation would be robust technique for confirming the antibody specificity. Further studies are warranted to verify the neuroprotective effects of CCR5 inhibition after experimental ICH in female mice.

CONCLUSIONS

The present study showed that CCR5 activation promoted NLRP1-dependent neuronal pyroptosis and neurological deficits, at least, in part, via the CCR5/PKA/CREB signaling pathway after experimental ICH in mice. CCR5 inhibition using MVC may provide a promising therapeutic strategy in the management of patients with ICH.

ARTICLE INFORMATION

Received October 29, 2020; final revision received July 11, 2021; accepted July 30, 2021.

Affiliations

Department of Neurosurgery, Guangxi Medical University Cancer Hospital, Nanning, China (J.Y.). Department of Neurosurgery, Second Affiliated Hospital, School of Medicine, Zhejiang University, Hangzhou, China (W.X.). Department of Biomedical Sciences, Burrell College of Osteopathic Medicine, Las Cruces, NM (C.L.). Department of Neurosurgery (L.H., J.H.Z.), Department of Physiology and Pharmacology (L.H., J.H.Z., J.T.), and Department of Anesthesiology (J.H.Z.), Loma Linda University, CA. Department of Rheumatism, First Affiliated Hospital of Guangxi Medical University, Nanning, China (J.W.). Department of Neurology, Tongji Hospital, Tongji Medical college, Huazhong University of Science and Technology, Wuhan, China (G.L.). Department of Neurosurgery, West China Hospital of Sichuan University, Chengdu, China (X.H.). Department of Neurology, The Third Xiangya Hospital of Central South University, Changsha, China (W.Z.).

Acknowledgments

Drs Yan, Xu, and Tang conceived the study; Drs Yan and Xu supervised and coordinated all aspects of the work; Drs Yan, Huang, Zhang, and Tang designed the experiments; Dr Yan, C. Lenahan, and Dr Huang wrote the paper; Drs Yan, Xu, Wen, Li, Hu, and Zheng performed the experiments, analyzed the data, and prepared the figures and tables; Drs Wen and Xu contributed with analytical tools.

Sources of Funding

This study was supported by grants from the National Natural Science Foundation of China (No. 82060225), Guangxi Natural Science Foundation (No. 2020JJA140117 and 2018JJA140243) to Dr Yan.

Disclosures

None.

Supplemental Materials

Expanded Materials and Methods
Supplemental Table I
Supplemental I–XVII
Data Set
References 18–38

REFERENCES

1. Liddle LJ, Ralhan S, Ward DL, Colbourne F. Translational intracerebral hemorrhage research: has current neuroprotection research ARRIVEd at a standard for experimental design and reporting? *Transl Stroke Res*. 2020;11:1203–1213. doi: 10.1007/s12975-020-00824-x
2. van Asch CJ, Luitse MJ, Rinkel GJ, van der Tweel I, Algra A, Klijn CJ. Incidence, case fatality, and functional outcome of intracerebral haemorrhage over time, according to age, sex, and ethnic origin: a systematic review and meta-analysis. *Lancet Neurol*. 2010;9:167–176. doi: 10.1016/S1474-4422(09)70340-0
3. Aronowski J, Zhao X. Molecular pathophysiology of cerebral hemorrhage: secondary brain injury. *Stroke*. 2011;42:1781–1786. doi: 10.1161/STROKEAHA.110.596718
4. McKenzie BA, Dixit VM, Power C. Fiery cell death: pyroptosis in the central nervous system. *Trends Neurosci*. 2020;43:55–73. doi: 10.1016/j.tins.2019.11.005
5. Yap JKY, Pickard BS, Chan EWL, Gan SY. The role of neuronal NLRP1 inflammasome in Alzheimer's disease: bringing neurons into the neuroinflammation game. *Mol Neurobiol*. 2019;56:7741–7753. doi: 10.1007/s12035-019-1638-7
6. Martin-Blondel G, Brassat D, Bauer J, Lassmann H, Liblau RS. CCR5 blockade for neuroinflammatory diseases–beyond control of HIV. *Nat Rev Neurol*. 2016;12:95–105. doi: 10.1038/nrneurol.2015.248
7. Joy MT, Ben Assayag E, Shabashov-Stone D, Liraz-Zaltsman S, Mazzitelli J, Arenas M, Abduljawad N, Kliper E, Korczyn AD, Thareja NS, et al. CCR5 Is a therapeutic target for recovery after stroke and traumatic brain injury. *Cell*. 2019;176:1143–1157.e13. doi: 10.1016/j.cell.2019.01.044
8. Zhou M, Greenhill S, Huang S, Silva TK, Sano Y, Wu S, Cai Y, Nagaoka Y, Sehgal M, Cai DJ, et al. CCR5 is a suppressor for cortical plasticity and hippocampal learning and memory. *Elife*. 2016;5:e20985. doi: 10.7554/eLife.20985
9. Kandel ER. The molecular biology of memory: cAMP, PKA, CRE, CREB-1, CREB-2, and CPEB. *Mol Brain*. 2012;5:14. doi: 10.1186/1756-6606-5-14
10. Wen AY, Sakamoto KM, Miller LS. The role of the transcription factor CREB in immune function. *J Immunol*. 2010;185:6413–6419. doi: 10.4049/jimmunol.1001829
11. Datta A, Sarmah D, Mounica L, Kaur H, Kesharwani R, Verma G, Veeresh P, Kotian V, Kalia K, Borah A, et al. Cell death pathways in ischemic stroke and targeted pharmacotherapy. *Transl Stroke Res*. 2020;11:1185–1202. doi: 10.1007/s12975-020-00806-z
12. Sborgi L, Rühl S, Mulvihill E, Pipercevic J, Heilig R, Stahlberg H, Farady CJ, Müller DJ, Broz P, Hiller S. GSDMD membrane pore formation constitutes the mechanism of pyroptotic cell death. *EMBO J*. 2016;35:1766–1778. doi: 10.15252/embj.201694696
13. Lin WP, Xiong GP, Lin Q, Chen XW, Zhang LQ, Shi JX, Ke QF, Lin JH. Heme oxygenase-1 promotes neuron survival through down-regulation of neuronal NLRP1 expression after spinal cord injury. *J Neuroinflammation*. 2016;13:52. doi: 10.1186/s12974-016-0521-y
14. Fann DY, Lee SY, Manzanero S, Tang SC, Gelderblom M, Chunduri P, Bernreuther C, Glatzel M, Cheng YL, Thundyil J, et al. Intravenous immunoglobulin suppresses NLRP1 and NLRP3 inflammasome-mediated neuronal death in ischemic stroke. *Cell Death Dis*. 2013;4:e790. doi: 10.1038/cddis.2013.326
15. Pittaluga A. CCL5-Glutamate cross-talk in astrocyte-neuron communication in multiple sclerosis. *Front Immunol*. 2017;8:1079. doi: 10.3389/fimmu.2017.01079

16. Cowell RM, Xu H, Galasso JM, Silverstein FS. Hypoxic-ischemic injury induces macrophage inflammatory protein-1alpha expression in immature rat brain. *Stroke*. 2002;33:795–801. doi: 10.1161/hs0302.103740
17. Offner H, Subramanian S, Parker SM, Afentoulis ME, Vandenbark AA, Hurn PD. Experimental stroke induces massive, rapid activation of the peripheral immune system. *J Cereb Blood Flow Metab*. 2006;26:654–665. doi: 10.1038/sj.jcbfm.9600217
18. Karampoor S, Zahednasab H, Amini R, Esghaei M, Sholeh M, Keyvani H. Maraviroc attenuates the pathogenesis of experimental autoimmune encephalitis. *Int Immunopharmacol*. 2020;80:106138. doi: 10.1016/j.intimp.2019.106138
19. Huang H, Zepp M, Georges RB, Jarahian M, Kazemi M, Eyol E, Berger MR. The CCR5 antagonist maraviroc causes remission of pancreatic cancer liver metastasis in nude rats based on cell cycle inhibition and apoptosis induction. *Cancer Lett*. 2020;474:82–93. doi: 10.1016/j.canlet.2020.01.009
20. Kravitz AV, Kreitzer AC. Striatal mechanisms underlying movement, reinforcement, and punishment. *Physiology (Bethesda)*. 2012;27:167–177. doi: 10.1152/physiol.00004.2012
21. Wang Z, Zhou F, Dou Y, Tian X, Liu C, Li H, Shen H, Chen G. Melatonin Alleviates intracerebral hemorrhage-induced secondary brain injury in rats via suppressing apoptosis, inflammation, oxidative stress, DNA damage, and mitochondria injury. *Transl Stroke Res*. 2018;9:74–91. doi: 10.1007/s12975-017-0559-x
22. Caracciolo L, Marosi M, Mazzitelli J, Latifi S, Sano Y, Galvan L, Kawaguchi R, Holley S, Levine MS, Coppola G, et al. CREB controls cortical circuit plasticity and functional recovery after stroke. *Nat Commun*. 2018;9:2250. doi: 10.1038/s41467-018-04445-9
23. Guan X, Wang Y, Kai G, Zhao S, Huang T, Li Y, Xu Y, Zhang L, Pang T. Cerebrolysin ameliorates focal cerebral ischemia injury through neuroinflammatory inhibition via CREB/PGC-1α pathway. *Front Pharmacol*. 2019;10:1245. doi: 10.3389/fphar.2019.01245
24. Lara LS, Vives D, Correa JS, Cardozo FP, Marques-Fernades MF, Lopes AG, Caruso-Neves C. PKA-mediated effect of MAS receptor in counteracting angiotensin II-stimulated renal Na+-ATPase. *Arch Biochem Biophys*. 2010;496:117–122. doi: 10.1016/j.abb.2010.02.005
25. Luo Y, Reis C, Chen S. nlrp3 inflammasome in the pathophysiology of hemorrhagic stroke: a review. *Curr Neuropharmacol*. 2019;17:582–589. doi: 10.2174/1570159X17666181227170053
26. Bai N, Zhang Q, Zhang W, Liu B, Yang F, Brann D, Wang R. G-protein-coupled estrogen receptor activation upregulates interleukin-1 receptor antagonist in the hippocampus after global cerebral ischemia: implications for neuronal self-defense. *J Neuroinflammation*. 2020;17:45. doi: 10.1186/s12974-020-1715-x
27. Liang Y, Jing X, Zeng Z, Bi W, Chen Y, Wu X, Yang L, Liu J, Xiao S, Liu S, et al. Rifampicin attenuates rotenone-induced inflammation via suppressing NLRP3 inflammasome activation in microglia. *Brain Res*. 2015;1622:43–50. doi: 10.1016/j.brainres.2015.06.008
28. Xie Y, Li YJ, Lei B, Kernagis D, Liu WW, Bennett ER, Venkatraman T, Lascola CD, Laskowitz DT, Warner DS, et al. Sex differences in gene and protein expression after intracerebral hemorrhage in mice. *Transl Stroke Res*. 2019;10:231–239. doi: 10.1007/s12975-018-0633-z
29. Yan J, Zuo G, Sherchan P, Huang L, Ocak U, Xu W, Travis ZD, Wang W, Zhang JH, Tang J. Ccr1 activation promotes neuroinflammation through ccr1/tpr1/erk1/2 signaling pathway after intracerebral hemorrhage in mice. *Neurotherapeutics: J Am Soc Exp NeuroTherapeutics*. 2020;17:1170–1183. doi: 10.1007/s13311-019-00821-5
30. Rolland WB, Lekic T, Krafft PR, Hasegawa Y, Altay O, Hartman R, Ostrowski R, Manaenko A, Tang J, Zhang JH. Fingolimod reduces cerebral lymphocyte infiltration in experimental models of rodent intracerebral hemorrhage. *Exp Neurol*. 2013;241:45–55. doi: 10.1016/j.expneurol.2012.12.009
31. Hang LH, Shao DH, Chen Z, Chen YF, Shu WW, Zhao ZG. Involvement of spinal CC chemokine ligand 5 in the development of bone cancer pain in rats. *Basic Clin Pharmacol Toxicol*. 2013;113:325–328. doi: 10.1111/bcpt.12099
32. Wang S, Zhang Z, Qian W, Ji D, Wang Q, Ji B, Zhang Y, Zhang C, Sun Y, Zhu C, et al. Angiogenesis and vasculogenic mimicry are inhibited by 8-Br-cAMP through activation of the cAMP/PKA pathway in colorectal cancer. *Onco Targets Ther*. 2018;11:3765–3774. doi: 10.2147/OTT.S164982
33. Luo Y, Fang Y, Kang R, Lenahan C, Gamdzyk M, Zhang Z, Okada T, Tang J, Chen S, Zhang JH. Inhibition of EZH2 (enhancer of zeste homolog 2) attenuates neuroinflammation via H3k27me3/SOCS3/TRAF6/NF-κB (trimethylation of histone 3 lysine 27/suppressor of cytokine signaling 3/tumor necrosis factor receptor family 6/nuclear factor-κB) in a rat model of subarachnoid hemorrhage. *Stroke*. 2020;51:3320–3331. doi: 10.1161/STROKEAHA.120.029951
34. Kar P, Agnihotri SK, Sharma A, Sachan R, Lal Bhatt M, Sachdev M. A protocol for stripping and reprobing of Western blots originally developed with colorimetric substrate TMB. *Electrophoresis*. 2012;33:3062–3065. doi: 10.1002/elps.201200333
35. Tokami H, Ago T, Sugimori H, Kuroda J, Awano H, Suzuki K, Kiyohara Y, Kamouchi M, Kitazono T; REBIOS Investigators. RANTES has a potential to play a neuroprotective role in an autocrine/paracrine manner after ischemic stroke. *Brain Res*. 2013;1517:122–132. doi: 10.1016/j.brainres.2013.04.022
36. Zhang C, Jiang M, Wang WQ, Zhao SJ, Yin YX, Mi QJ, Yang MF, Song YQ, Sun BL, Zhang ZY. Selective mGluR1 negative allosteric modulator reduces blood-brain barrier permeability and cerebral edema after experimental subarachnoid hemorrhage. *Transl Stroke Res*. 2020;11:799–811. doi: 10.1007/s12975-019-00758-z
37. Liu H, Hua Y, Keep RF, Xi G. Brain ceruloplasmin expression after experimental intracerebral hemorrhage and protection against iron-induced brain injury. *Transl Stroke Res*. 2019;10:112–119. doi: 10.1007/s12975-018-0669-0
38. Ocak U, Ocak PE, Huang L, Zuo G, Yan J, Hu X, Song Z, Zhang JH. Inhibition of PAR-2 attenuates neuroinflammation and improves short-term neurocognitive functions Via ERK1/2 signaling following asphyxia-induced cardiac arrest in rats. *Shock*. 2020;54:539–547. doi: 10.1097/SHK.0000000000001516